the structural bottlenecks can be described as tetraradicaloid with three localized unpaired electrons and a fourth delocalized unpaired electron in an quasi-planar allyl-like fragment. The occurrence of the many different photorearrangement products in the precalciferol reaction network is completely rationalized by the many possible spin recouplings that can occur in this tetraradicaloid as it emerges on the ground-state surface at the conical intersection. Thus the main branches of the ergosterol photochemistry (leading to lumisterol and tachysterols) can be rationalized via pathways involving the passage through these conical intersections.

Acknowledgment. This work was supported by the SERC (UK) under grant numbers GR/F 48029, 46452, and GR/G 03335. All ab initio computations were carried using MC-SCF programs that are available in GAUSSIAN 91.[5]

The Conformations of Proline-Linked Donor-Acceptor Systems

Scott F. Sneddon*,† and Charles L. Brooks III‡

Contribution from Pfizer Central Research, Groton, Connecticut 06340, and the Department of Chemistry, Carnegie Mellon University, Pittsburgh, Pennsylvania 15213.
Received December 27, 1991

Abstract: We have carried out a simulation study of the stable conformations of Pro–Pro peptides in solution, and of Pro_n peptides (where n = 1–4) in a dielectric continuum model, to explain the observed electron-transfer rates in proline-linked donor–acceptor systems studied by Isied and Vassilian.[1] They found that the rate of electron transfer in proline-linked donor–acceptor systems decreases by the expected amount for Pro_2 versus Pro_1, but for Pro_3 and Pro_4 the rate increases, with Pro_4 having the fastest transfer rate of the peptides studied. This finding suggests that conformational flexibility in the longer peptides enables the donor and acceptor to reach short transfer distances, resulting in the faster transfer rate. We have performed conformational free energy simulations to determine the free energy barriers for transitions of the backbone degrees of freedom of Pro–Pro peptides in solution. From the stable structures found we have carried out simulations of the Pro_1-to-Pro_4-linked donor–acceptor systems to determine the structural changes that best explain the observed trend in the electron-transfer rates. We found that the proline secondary structures poly(Pro)I and poly(Pro)II cannot explain the trend in transfer rates and that, instead, transitions of the ψ backbone dihedral from an extended to an α conformation can give short enough transfer distances to explain the experimental rates. Our analysis suggests that transitions of the backbone ψ dihedral angle represent a significant mechanism for conformational change in proline peptides.

In this paper we discuss the influence of conformational flexibility on the rate and pathway of electron transfer in proline-linked donor–acceptor systems. Experimental studies have shown that the rate of transfer is not a simple function of the length of the peptide joining the donor and acceptor.[1,2] Rather, the rate first decreases with chain length and then begins to increase as the chain is lengthened (Table I). Since the covalent through-bond path increases with chain length, there can be two arguments to explain this observation. Either the longer chain can fold back on itself to bring the donor and acceptor closer or through-bond coupling becomes more efficient as the chain is lengthened.[3] In their first studies of this system Isied and Vassilian discussed the former cause and suggested that a conformational change to the poly(Pro)I structure[4,5] might explain the faster rates of the Pro_3 and Pro_4 peptides. More recently, they have discussed the latter cause, attributing the change in rate to more efficient electronic coupling for the amide group in the longer peptides (specifically in the all cis conformation of the backbone).[3] Our calculations of the tunneling barrier height of amides do not support a significant change in the electronic coupling for the two conformations, so we have explored the role of conformational change in enhancing the rate in the longer peptides.

Proline is a unique amino acid in two important ways. First, the covalent link between C^α and the amino nitrogen greatly reduces the rotational freedom of the backbone ϕ angle. Second, the lack of an amide proton makes the cis and trans conformations of the ω dihedral closer in free energy than in all other amino acids.[6,7] The dihedral angles ϕ, ψ, and ω, are shown in proline. Proline peptides adopt two types of regular backbone structure characterized by the value of ω. The right-handed helical form, poly(Pro)I, has all cis peptide bonds, while for the left-handed

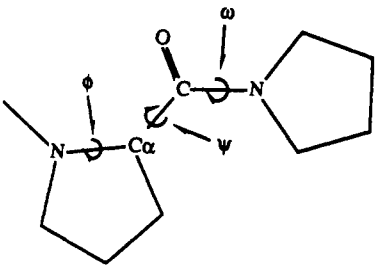

helical form of poly(Pro)II the peptide bonds are trans. In both of these conformations the ψ dihedral is in the extended, or β, conformation.[4] At pH 7 the all-trans poly(Pro)II is the more stable species.[6,7]

To determine how proline peptides can change conformation we computed gas-phase potential energy surfaces for both backbone degrees of freedom in proline: ψ and ω. We found that each dihedral has two stable minima: the cis and trans conformation of the ω dihedral and the α and β conformations of the ψ dihedral. We used potential of mean force (pmf) calculations to characterize the free energy for transitions between these stable structures in aqueous solvent. We found that gas-phase calculations that em-

† Pfizer Central Research.
‡ Carnegie Mellon University.

(1) Isied, S. S.; Vassilian, A. *J. Am. Chem. Soc.* **1984**, *106*, 1732–1736.
(2) Isied, S. S.; Vassilian, A. *J. Am. Chem. Soc.* **1984**, *106*, 1726–1732.
(3) Isied, S. S. In *200th ACS National Meeting*; Washington D.C., 1990; p 103.
(4) Richardson, J. S. *Adv. Protein Chem.* **1981**, *34*, 167–339.
(5) Creighton, T. E. *Proteins, Structures and Molecular Properties*; W. H. Freeman and Co.: New York, 1983.
(6) Thomas, W. A.; Williams, M. K. *J. Chem. Soc., Chem. Commun.* **1972**, 994.
(7) Evans, C. A.; Rabenstein, D. L. *J. Am. Chem. Soc.* **1974**, *96*, 7312–7317.

0002-7863/92/1514-8220$03.00/0

Table I. Rates and Thermodynamics of Electron Transfer for Pro_n-Linked DA Systems[a]

linker	rate[b] ($\times 10^5$/s)	ΔH_{react} (kcal/mol)	ΔS_{react} (eu)	ΔG_{react} (kcal/mol)
Pro_1	10.4	19.7 ± 1.1	−16 ± 4	22.8 ± 2.3
Pro_2	0.64	18.0 ± 1.9	−20 ± 6	24.6 ± 3.7
Pro_3	5.6	14.5 ± 1.1	−29 ± 4	23.2 ± 2.3
Pro_4	14.0	10.0 ± 0.7	−43 ± 3	22.9 ± 1.6

[a] Results taken from the work of Isied and Vasillian.[1] [b] Rates determined at 24.8 ± 0.05 °C.

ployed a dielectric constant of 80 (to account for solvent screening of charge—charge interactions) gave results that agreed qualitatively with the solvent simulations. We then generated structures for the peptides with ψ and ω each in their two possible stable minima. Each of these structures was subjected to gas-phase molecular dynamics, using a dielectric constant of 80, and the average donor–acceptor distance and the fluctuations in this distance were computed.

We then considered the difference in the tunneling barrier for the through-solvent versus through-peptide pathways to determine the maximum distance for through-solvent transfer to match the observed rate. The only structures predicted to transfer electrons at the observed rate have the ψ dihedral in the α conformation. We also found that the regular secondary structures of the peptide, poly(Pro)I and poly(Pro)II, yield the longest donor–acceptor distances of the conformations studied and are therefore not likely candidates for the structures from which transfer takes place. These results highlight the importance of transitions of the backbone ψ dihedral, in addition to the recognized transitions of the ω angle, as an important mechanism for conformational change in proline containing peptides.

Computational Details

The Model System. The model system used in the simulations consisted of proline mono- through tetrapeptides with donor and acceptor systems attached. The donor and acceptor models were $(NH_3)_5{}^{III}Fe$-pyridine and $(NH_3)_5Fe^{II}$ groups used to block the N- and C-terminal ends of the peptide, respectively. The bond, angle, dihedral, and van der Waals energy parameters for these groups were taken from analogous CHARMM[8] parameters for heme iron and its ligands and are similar to other parameters for such groups given in the literature (Table II). The atomic charges were determined from an SCF calculation of an $Fe(NH_3)_6$ cluster using the STO-3G basis set[9,10] and the G90 computer program[11] and showed significant delocalization of the metal charge onto the ligands.[12] It is important to note that the properties we will discuss should not rely heavily on details of the donor or acceptor structure. We only seek to model the gross features of a charged metal–ligand system bound to each end of the peptide. Since the iron atoms are bonded directly to the peptide, the iron–iron distance should depend mostly on the peptide conformation and not on the internal structure of the metal–ligand system itself. In light of the similarity of the metal ligand parameters shown in Table II[13] we feel the current parameterization is sufficient for this study.

Characterizing the Extended Peptides. The peptides were built from internal coordinates with ψ at 180, ω at 180°, and ϕ −75°. A simulation was run to obtain an Fe–Fe distance distribution for each of the peptides. Each peptide was simulated for 15 ps using a 1.5 fs timestep. Velocities were assigned as necessary to maintain a temperature of 300 K. Nonbonded interactions were not truncated (∞ cutoffs), and a dielectric constant of 80 was used to account for screening of Coulombic interactions by aqueous solvent. Once this unconstrained probability distribution was generated, it was used as the central distance of five umbrella sampling windows in the Fe–Fe distance.[14-16] Potentials of mean force spanning ~5 Å in Fe–Fe distance were generated for each of the proline peptides.

Table II. Potential Energy Parameters Used To Simulate the Liganded Iron[a]

(a) Bond Parameters

bond type	force constant (kcal/mol Å^2)	bond length (Å)
Fe(II)–N	65.0	2.0
Co(III)–N	143.9	1.925
Ni(II)–N	48.9	2.1
Cu(II)–N	61.2	2.03

(b) Bond Angle Parameters

angle type	force constant (kcal/mol radian^2)	bond angle (radians)
N–Fe–N	50	1.5711
Fe–N–H	35	1.911
N–Co–N	48.9	1.5711
N–Ni–N	21.6	1.5711
Co–N–H	14.4	1.911

[a] Parameters for noniron atoms were taken from the collected data by Hancock.[13]

ψ, ω Maps. The gas-phase ψ, ω map was generated by the following procedure. A blocked Pro–Pro peptide was built from standard internal coordinates with ψ and ω set to −180° and ϕ set to −75° (the blocking groups were an acetyl group at the N terminus and an *N*-methyl amide at the C-terminus to give an extra amide group at each end). The energy of the molecule was minimized, subject to a dihedral restraint on both ψ and ω, for 150 steps or until the gradient in the energy fell below 0.1 kcal/mol. The values of ψ, ω, and the minimized energy were stored to a file, and the minimum of the dihedral restraint was moved to −160°. This procedure was repeated until an 18 × 18 grid of minimum energies was computed for each combination of ψ and ω. The alanine ϕ, ψ map was generated using an alanine residue blocked with an acetyl group at the N-terminus and *N*-methyl amide at the C-terminus and varying the ϕ,ψ dihedral angles.

ψ, ω Transitions in Solution. Each of the potentials of mean force was computed using an acetyl and *N*-methyl amide blocked Pro–Pro peptide. A periodic box of 216 TIP3 water molecules was used;[17] the edge length of the box was 18.856 Å. The potentials of mean force were produced using harmonic dihedral angle restraints that allowed the dihedral to undergo rms fluctuations of approximately ±10° (a force constant of about 14 kcal/mol·rad^2 was used in the restraining potential). The reaction coordinates were defined as follows: β-trans → α-trans, ω = 180, ψ = 160° to −60° in 12 windows; β-trans → β-cis, ψ = 160°, ω = 200° to −20° in 12 windows; β-cis → α-cis, ω = 0°, ψ = 160° to −60° in 12 windows. All windows were spaced at 20° increments, with the other dihedral (ω in the $\alpha \rightarrow \beta$ transitions, and ψ in the cis → trans transitions) unrestrained. The dihedral angle probability distribution at each value of the reaction coordinate was produced from a simulation with 15 ps of equilibration dynamics, followed by 75 ps of production dynamics during which coordinates were saved every five steps. Because the barriers to transition were fairly large, there were some regions of the reaction coordinate where the probability distributions did not overlap sufficiently; in these cases extra umbrella sampling windows were added. For the β-trans → α-trans reaction coordinate two extra windows were added, one at the top of the barrier ($\psi \sim 20°$) and one on the steep portion of the pmf between the barrier and β conformation. The β-trans and β-cis pmf required a single extra window at the top of the barrier, ω = 90°. To ensure sampling in these regions, the force constant of the umbrella restraint was doubled.

Influence of ψ and ω Transitions on the Donor–Acceptor Distance in Proline-Linked D–A Systems. The model for the donor and acceptor groups was the same as used to characterize the extended peptides; the simulations were carried out in the gas phase using a dielectric constant of 80. From each starting conformation 7.5 ps of equilibration dynamics was run followed by 15 ps of production dynamics. The dynamics were

(8) Brooks, B. R.; Bruccoleri, R. E.; Olafson, B. D.; States, D. J.; Swaminathan, S.; Karplus, M. *J. Comput. Chem.* **1983**, *4*, 187–217.
(9) Hehre, W. J.; Stewart, R. F.; Pople, J. A. *J. Chem. Phys.* **1969**, *51*, 2657–2664.
(10) Pietro, W. J.; Hehre, W. J. *J. Comput. Chem.* **1983**, *4*, 241–251.
(11) Frisch, M. J.; Head-Gordon, M.; Trucks, G. W.; Foresman, J. B.; Schlegel, H. B.; Raghavachari, K.; Robb, M.; Binkley, J. S.; Gonzalez, C.; Defrees, D. J.; Fox, D. J.; Whiteside, R. A.; Seeger, R.; Melius, C. F.; Baker, J.; Martin, R. L.; Kahn, L. R.; Stewart, J. J. P.; Topiol, S.; Pople, J. A. *Gaussian 90, Revision F*; Gaussian, Inc.: Pittsburgh, PA, 1990.
(12) Hoops, S. C.; Anderson, K. W.; Merz, K. M., Jr. *J. Am. Chem. Soc.* **1991**, *113*, 8262–8270.
(13) Hancock, R. D. *Prog. Inorg. Chem.* **1989**, *37*, 187–291.
(14) Northrup, S. H.; Pear, M. R.; Lee, C. Y.; McCammon, J. A.; Karplus, M. *Proc. Natl. Acad. Sci. U.S.A.* **1982**, *79*, 4035–4039.
(15) Brooks, C. L., III; Karplus, M.; Pettitt, B. M. *Proteins: A Theoretical Perspective of Dynamics, Structure and Thermodynamics*; Wiley and Sons: New York, 1988; Vol. 75, pp 75–87.
(16) Tobias, D. J.; Sneddon, S. F.; Brooks, C. L., III *J. Mol. Biol.* **1991**, *216*, 783.
(17) Jorgensen, W. L.; Chandrasekhar, J.; Madura, J.; Impey, R. W.; Klein, M. L. *J. Chem. Phys.* **1983**, *79*, 926–935.

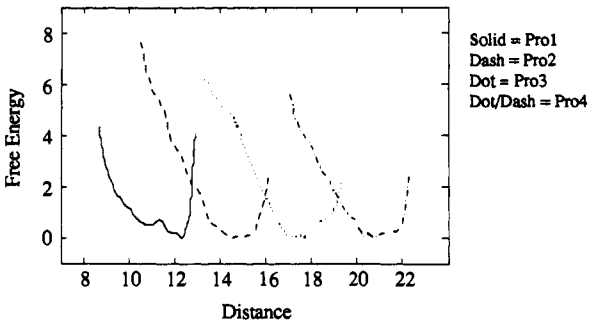

Figure 1. Potentials of mean force (free energy profiles) for changing the Fe–Fe distance in the extended conformation of Pro1 through Pro4.

Table III. Average Distances and Fluctuations, Extended Conformations

peptide	av distance (Å)	RMS fluctuation (Å)	peptide	av distance (Å)	RMS fluctuation (Å)
Pro1	11.5	0.5	Pro3	17.5	0.5
Pro2	14.7	0.4	Pro4	21.0	0.4

propagated by Langevin dynamics with a bath temperature of 300 K and a frictional coefficient of 30 ps^{-1}.[18] The average donor–acceptor distance and distance fluctuations were obtained from the production dynamics where structures were saved every 10 steps.

Results/Discussion

Characterizing the Extended Peptides. The first study in the series involved the computation of probability distributions for the Fe–Fe distance in poly(Pro)II forms of the $(NH_3)_5$Fe-Pyr-Pro_1-Fe$(NH_3)_5$ through $(NH_3)_5$Fe-Pyr-Pro_4-Fe$(NH_3)_5$ systems. These pmf's are shown together in Figure 1. The most stable Fe–Fe distance increases by increments of 3 Å for the addition of each proline, as expected (Table III). The pmf's also suggest that the Fe–Fe distance in Pro_3–Pro_4 cannot reach small values without crossing a barrier of at least 6 kcal/mol. These peptides can change their end–end distance by rotation of the two backbone dihedral angles ψ and ω. The free energy barriers for these rotations and the change in Fe–Fe distance that results are the topic of the next three sections.

ψ, ω Maps. Ramachandran, or ϕ, ψ, maps[19,20] have been used to identify the stable conformations of polypeptide chains in terms of the backbone dihedral angles in non-proline peptides. The Ramachandran map for non-glycine residues has two dominant stable regions of ϕ and ψ termed the α_R (α_{Right}) and β regions (Figure 2); there is also a slightly stable α_L (α_{Left}) region. These features are illustrated in Figure 2 for an alanine peptide blocked with an acetyl group at the N-terminus and *N*-methyl amide at the C-terminus. The α_R and β conformations differ by ~180° rotation about the ψ dihedral, and α_R and α_L differ by ϕ rotation. Most residues in proteins and peptides are either in α_R or β conformation.[5] In proline peptides the ϕ dihedral is held somewhat rigidly by the covalent connection between C_α and N, changing only slightly for "up" to "down" transition in the five-member prolyl ring. In proline residues ψ and ω are the relevant backbone dihedral angles, and we have constructed a ψ, ω map to show the stable conformations in proline peptides. The contour surface of these energies is shown in Figure 3. There are four minima on this surface corresponding to combinations of the two stable conformations of ψ and ω. We will discuss transitions between these minima at some length, so it is useful to adopt a nomenclature for the regions of the surface. The broad minima at ψ = 140°, ω = 180° will be termed the β-trans conformation because

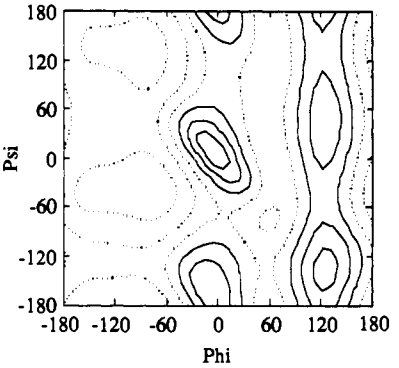

Figure 2. Map of energies as a function of the ϕ and ψ backbone dihedral angles for alanine. Computed from the CHARMM potential energy function using a dielectric constant of 80. Contours are at 2 kcal/mol intervals, dotted contours are the lowest energy regions, and solid lines are the highest energy regions.

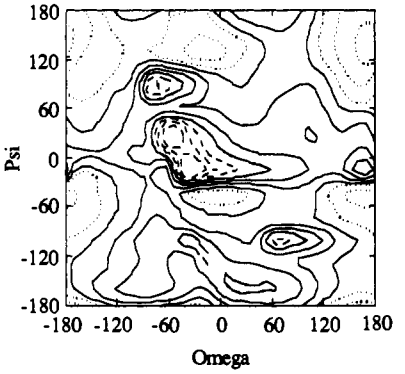

Figure 3. Map of energies as a function of the ψ and ω backbone dihedral angles for proline. Computed from the CHARMM potential energy function using a dielectric constant of 1. Contour lines are at 5 kcal/mol intervals, dotted lines are low energy contours, followed by solid line, and the dashed lines are the highest in energy.

ψ is in the β-region of the ϕ, ψ map, and the peptide bond is trans. The region at ψ = 140°, ω = 0° will be called the β-cis conformation, and the regions at ψ = −40°, ω = 180°, and ψ = −50°, ω = 0° will be termed α-trans and α-cis, respectively. By counting contour lines, the barrier for β-trans → β-cis is approximately 22 kcal/mol for the trans → cis transition and approximately 17 kcal/mol for the β-cis → β-trans transition; these values are in reasonable agreement with experimental estimates of the cis → trans barrier.[21] The barrier to transition from β-trans → α-trans is much larger, 27 kcal/mol for a path that avoids the maximum near ω = 170°, ψ = 20°. For the β-cis → α-cis transition the linear path in ψ would cross a very high barrier of ~50 kcal/mol, while a more convoluted path around the double maximum near ω = −60°, ψ = 0° crosses a barrier of approximately 20 kcal/mol. The barrier between ω = cis and ω = trans arises primarily from dihedral angle energy changes and should not be greatly affected by solvent polarity. In contrast, the barriers separating ψ = β from ψ = α arise mostly from electrostatic repulsion between backbone carbonyl groups, so dielectric screening in polar solvents should lower these barriers.

To better understand the influence of solvent polarity on the conformational energy, the ψ, ω map was generated again using a dielectric constant of 80 in the CHARMM electrostatic energy term. The surface that results from this calculation is quite different from Figure 3 and is shown in Figure 4. This surface has the same four dihedral minima as the dielectric 1 surface but has significantly different barriers separating them. The barrier between β-cis and β-trans is about 17–18 kcal/mol on this surface, similar to the previous value, because the dihedral angle energy term is unaffected by changes in dielectric constant. The most

(18) McCammon, J. A.; Harvey, S. C. *Dynamics of Proteins and Nucleic Acids*; Cambridge University Press: Cambridge, 1987.
(19) Ramachandran, G. N.; Sasisekharan, V. *Adv. Protein Chem.* **1968**, *23*, 283–437.
(20) Zimmerman, S. S.; Pottle, M. S.; Némethy, G.; Scheraga, H. A. *Macromolecules* **1977**, *10*, 1–9.
(21) Cheng, H. N.; Bovey, F. A. *Biopolymers* **1977**, *16*, 1465–1472.

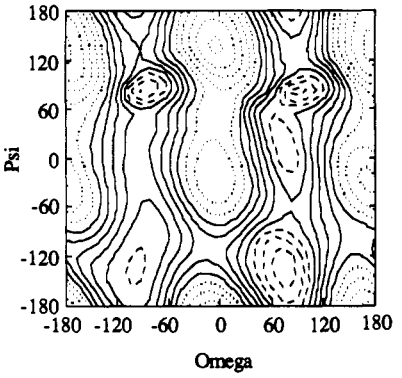

Figure 4. Map of energies as a function of the ψ and ω backbone dihedral angles for proline. Computed from the CHARMM potential energy function using a dielectric constant of 80. Contour lines are at 2 kcal/mol intervals, the dotted lines are the lowest energy regions, and the dashed lines are the highest energy regions.

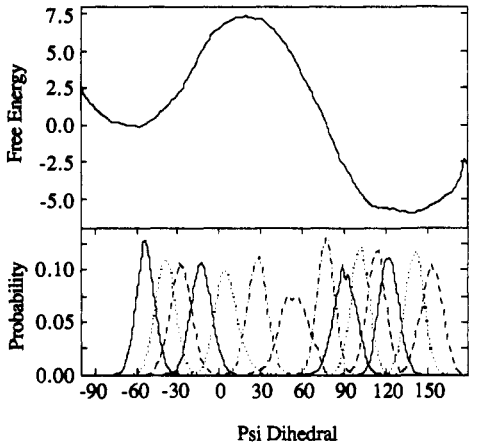

Figure 5. Potential of mean force and probabilities for the β-trans → α-trans transition in solvent.

significant changes in the surface occur in the regions between β-cis and α-cis and between β-trans and α-trans. Here, the barriers are much lower; the lowest energy $\alpha \rightarrow \beta$ path is a direct ψ transition (with a barrier 9 kcal/mol), and the α-minima are broader.

ψ, ω Transitions in Solution. To evaluate the accuracy of the ψ, ω map (computed with a dielectric constant of 80) we performed potential of mean force calculations in aqueous solvent. These simulations yield free energy profiles for reaction coordinates that take the system between stable conformations on the gas-phase (dielectric = 80) surface. For this part of the study we used umbrella sampling along a reaction coordinate in ψ or ω to connect β-trans to α-trans, β-trans to β-cis, and β-cis to α-cis. By comparing the results of these calculations, which were performed with explicit solvent, with the predictions from the dielectric 80 ψ, ω surface, we can assess whether the stable minima on the ψ, ω surface also exist in solution.

The potential of mean force for the β-trans → α-trans reaction coordinate, along with the associated dihedral probabilities, is shown in Figure 5. The significant features of the pmf include the following: stable minima at $\psi \sim -60°$ and $+140°$, a barrier separating these conformations at $\psi \sim 20°$, a $\beta \rightarrow \alpha$ barrier of approximately 12 kcal/mol, an $\alpha \rightarrow \beta$ barrier of approximately 7 kcal/mol, and thus a free energy difference of ~5 kcal/mol. This agrees quite well with the quantities predicted from the ψ, ω dielectric 80 map (Figure 4).

The potential of mean force along the reaction coordinate connecting β-trans and β-cis is shown in Figure 6 along with the associated dihedral probabilities.

The pmf shows the expected minima at $\omega = 0°$ and 180°, with a barrier of ~18 kcal/mol at $\omega = 90°$. The minima are close in free energy with the cis conformation approximately 2 kcal/mol

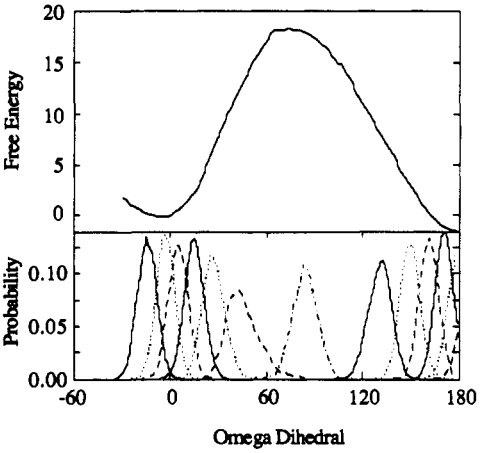

Figure 6. Potential of mean force and probabilities for the β-trans → β-cis transition in solvent.

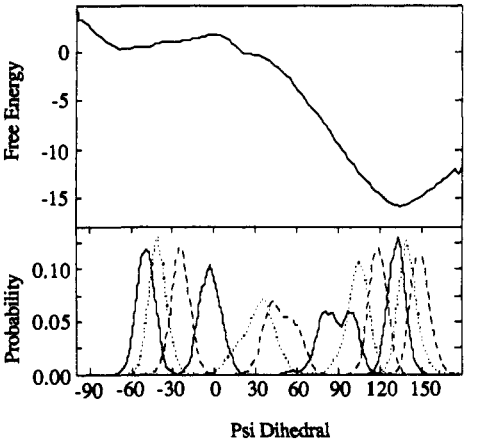

Figure 7. Potential of mean force and probabilities for the β-cis → α-cis transition in solvent.

higher in free energy than trans. The computed barrier height, and the free energy difference between cis and trans conformations are in good agreement with the experimental estimates.[6,7,21] The barrier height on the gas phase (dielectric = 80) ψ, ω surface was also 18 kcal/mol, though no significant energy difference between cis and trans conformations was predicted.

The final potential of mean force, that connecting β-cis and α-cis, is shown in Figure 7. In comparison to the β-trans → α-trans transition, the conformation at $\psi = -60°$ is only marginally stable, the barrier at $\psi = 20°$ is less than 2 kcal/mol. The barrier for the β-cis → α-cis transition is ~17 kcal/mol. The smaller stability of the α-cis conformation (compared to α-trans) is also seen in the dielectric 80 ψ, ω map where the barrier is ~3 kcal/mol. The barrier for the β-cis to α-cis transition on the ψ, ω surface is smaller than in solvent (~9 kcal/mol versus ~17 kcal/mol).

The solvent potentials of mean force and the dielectric 80 ψ, ω map indicate that Pro–Pro peptides have kinetically stable conformations when ψ is α. These conformations are in addition to the recognized secondary structures of proline, poly(Pro)I, and poly(Pro)II, which have ψ in the β conformation and differ by cis–trans isomerization of ω. Since the cis and trans isomers are close in free energy, there will be significant populations of both cis and trans isomers at equilibrium. There will be a much smaller equilibrium population of α isomers because they are higher in free energy. However, once formed, the α-trans isomer will exist for a significant amount of time because of the barrier of ~7 kcal/mol separating it from the β-trans isomer. When the peptide bond is cis, the α-conformation is only marginally stable (~2 kcal/mol), and the α-cis conformation should be short-lived. Furthermore, the 15 kcal/mol barrier separating β-cis and α-cis and the 12 kcal/mol barrier separating β-trans and α-trans are both smaller than the 18 kcal/mol barrier separating β-trans from

Table IV. Average Distances and Fluctuations, $\psi = \alpha$ Conformations

peptide	av distance (Å)	RMS fluctuation (Å)	peptide	av distance (Å)	RMS fluctuation (Å)
Pro2α1	11.0	0.4	Pro4α2	7.2	0.4
Pro3α1	9.6	1.0	Pro4α3	14.7	0.6
Pro3α2	10.6	0.9	Pro4α12	8.6	0.5
Pro3α12	10.7	0.7	Pro4α13	5.3	0.3
Pro4α1	9.0	0.5	Pro4α23	7.3	0.4
			Pro4α123	12.9	0.4

Table V. Average Distances and Fluctuations, ω = cis Conformations

peptide	av distance (Å)	RMS fluctuation (Å)	peptide	av distance (Å)	RMS fluctuation (Å)
Pro2c1	10.9	0.5	Pro4c3	9.8	0.4
Pro3c1	13.0	0.5	Pro4c12	12.4	0.6
Pro3c2	11.0	0.8	Pro4c13	9.0	0.5
Pro3c12	12.8	0.3	Pro4c23	16.9	0.4
Pro4c1	17.2	0.4	Pro4c123	16.7	0.3
Pro4c2	9.6	1.2			

β-cis. Therefore, while the equilibrium population of α isomers is smaller than that of cis isomers, $\beta \rightarrow \alpha$ interconversions occur more rapidly than trans $\rightarrow$ cis interconversions. Since the activation free energy for electron transfer[1] is several kcal/mol larger than the computed barrier for transition of either ψ or ω (Table I), conformational change of either dihedral could occur on the time scale of the electron transfer. The kinetically stable α-isomers are another means by which the electron-transfer distance might change in proline-linked donor–acceptor systems. The change in donor–acceptor distance for trans $\rightarrow$ cis and $\beta \rightarrow \alpha$ transitions is the subject of the next section.

The Influence of ψ and ω Transitions on the Donor–Acceptor Distance in Proline-Linked D–A Systems. To understand how changes in the ψ and ω dihedral angles can change the donor–acceptor distance in proline-linked electron-transfer systems, we have performed a series of molecular dynamics simulations on models of D-Pro$_n$-A where $n = 1 \rightarrow 4$. For each value of n, all possible cis and all possible α conformations were simulated, including double and triple α and cis but no α-cis combinations. For the Pro$_2$ peptide the conformations are simply $\psi = \alpha$ and ω = cis for the single set of dihedral angles between the two proline residues. For Pro$_3$ there are two sets of ψ, ω dihedrals, and both single and double dihedral rotations were made. In Pro$_4$ there are three dihedral angle pairs, and all single, double, and triple dihedral rotations were considered. The nomenclature used to discuss the different conformers is specified by first giving the name of the peptide (Pro$_2$, Pro$_3$, or Pro$_4$) followed by either α or c to signify conformers in ψ or ω and a set of numbers to indicate which dihedrals were altered. For example, Pro3α1 specifies the Pro$_3$ peptide with the ψ angle of the first residue in α conformation, Pro3c1 specifies the same peptide with the ω angle of the backbone linking the first and second residues in cis conformation. The multiple dihedral species are signified with multiple dihedral numbers, e.g., Pro4α13 has the first and third ψ angles in α conformation.

The averages and fluctuations in the donor–acceptor distance are tabulated in Tables IV and V.

Starting with Pro$_2$ we see that, in comparison to an average D–A distance of 14.7 Å in the β-trans conformation, the α-conformation has an average D–A distance of 11.0 Å and the cis conformation has an average D–A distance of 10.9 Å. Thus, for Pro$_2$ we expect similar changes in the D–A distance for rotation of either ψ and ω. In Pro3 (where the β-trans D–A distance is 17.5 Å) the shortest single dihedal structure (Pro3α1) yields a D–A distances of 9.6 Å, while the shortest single cis structure yields a distance of 10.9 Å. The double dihedral structures also result in D–A distances that are shorter for $\psi = \alpha$ transitions than for ω = cis transitions. Here we see the first evidence that a single torsional transition can bring the D–A distance to within 10 Å and that α-transitions result in shorter D–A distances than any of the cis transformations. Furthermore, the Pro3c12 conformation, which corresponds to poly(Pro)I secondary structure, has among the longer D–A distances, at 12.8 Å.

Table VI. Donor–Acceptor Distances Required To Reproduce the Observed Rates

peptide	ratio of rates	tunnel expression	peptide	ratio of rates	tunnel expression
Pro$_1$	unity	exp(−0.9 × 11.5)[a]	Pro$_3$	0.5	exp(−1.4 × 8.0)[b]
Pro$_2$	0.06	exp(−0.9 × 14.7)[a]	Pro$_4$	1.3	exp(−1.4 × 7.2)[b]

[a] The factor of 0.9 (Å^{-1}) reflects the tunneling barrier of the peptide group;[22,23,25] the distances 11.5 and 14.7 (Å) come from the simulations of the extended Pro$_1$ and Pro$_2$ peptide presented in this section. This increment of distance, with the predicted barrier height, exactly reproduces the ratio of rates between Pro$_1$ and Pro$_2$. [b] The factor of 1.4 (Å^{-1}) reflects the tunneling barrier in water;[22,23,25] the distances 8.0 and 7.2 (Å) are the longest that will give the observed rates for transfer through water.

In Pro$_4$, where the β-trans D–A distance is 21.0 Å, there are several conformations that yield very short D–A distances (less than 10 Å). The structure Pro4α2 yields the shortest single dihedral D–A distance of any of the peptides studied. Of the double cis dihedral structures only Pro4c13 gives a distance less than 10 Å (9.0 Å), while three of the double α-dihedral structures give distances at least this short. Here, Pro4α12 gives a D–A distance of 8.6 Å, and Pro4α13 and Pro4α23 give the remarkably short distances of 5.3 and 7.3 Å, respectively. Again it is interesting that the triple cis (Pro4c123), or poly(Pro)I, structure has one of the longest transfer distances at 16.7 Å.

In summary, ψ dihedral transitions from β to α have the largest influence on the D–A distance, and the poly(Pro)I structures for Pro$_3$ and Pro$_4$ do not yield short D–A distances. In the case of Pro$_3$ the α1 conformation has the shortest D–A distance, while for Pro$_4$ short D–A distances occur in Pro4α2 and the double dihedral structures Pro4α13 and Pro4α23.

To determine the D–A distances that must be reached by the longer peptides so that their transfer rates can match and exceed Pro$_1$ and Pro$_2$ we considered the variation in rates and the difference between through peptide and through solvent transfer. According to Marcus theory,[22] the distance dependence of the transfer rate can be expressed as exp($-\zeta r$), where ζ depends on the medium separating the donor and acceptor. In the extended conformation the line-of-site pathway for transfer will be a through-peptide path. When the peptide folds back to reach shorter distances, the pathway will be through-solvent (or through and inner sphere mechanism if the distance is very small). Our previous studies,[23,24] along with experimental work,[22] suggest that the decay constant, ζ, for tunneling through the peptide backbone is ~0.9 Å^{-1}, while for tunneling through water the decay constant is ~1.4 Å^{-1}.[22,25] Because the tunneling barrier for water is higher than for the peptide backbone, the through-solvent pathway will have a more rapid distance decay than the through-peptide path. The Pro$_3$ and Pro$_4$ peptides must therefore reach distances that are shorter than Pro$_2$ and Pro$_1$ for their rates to be comparable. Table VI summarizes the rates of transfer for these peptides and provides an estimate of the distance required for Pro$_3$ and Pro$_4$ to transfer electrons through solvent at the observed rates. From the data in Table VI we see that for the Pro$_3$ and Pro$_4$ peptides to transfer at the observed rates they must be able to reach donor–acceptor distances of 8.0 and 7.2 Å, respectively. The Pro$_2$ peptide can reach donor–acceptor distances of 11 Å by rotation of either ψ or ω, but the greater tunneling barrier for the through-water pathway leads to smaller rates for these structures than is achieved in the extended conformation. The extended Pro$_2$ conformation gives a coupling of exp(−0.9 × 14.7) = 1.8 × 10^{-6},

(22) Marcus, R. A.; Sutin, N. *Biochim. Biophys. Acta* **1985**, *811*, 265–322.
(23) Sneddon, S. F.; Morgan, R. S.; Brooks, C. L., III *Biophys. J.* **1988**, *53*, 83–89.
(24) Sneddon, S. F.; Brooks, C. L., III *Int. J. Quant. Chem. Quant. Biol. Symp.* **1988**, *15*, 23–32.
(25) Alexandrov, I. V.; Khairutdinov, R. F.; Zamaraev, K. I. *Chem. Phys.* **1978**, *32*, 123–141.

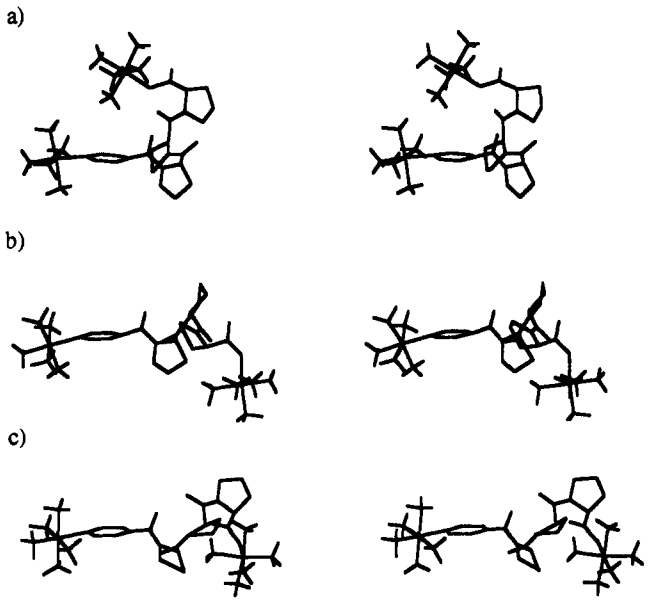

Figure 8. Stereoplots of the Pro3α1 (a), Pro_3 extended (poly(Pro)II) (b), and Pro_3 all-cis (poly(Pro)I) (c) structures.

whereas the through-water pathway gives a coupling of $\exp(-1.4 \times 11.0) = 2.1 \times 10^{-7}$, thus, transfer most likely occurs from the extended conformation. The predicted ratio of rates for Pro_1 and Pro_2 agrees very well with the experimental rate given in Table I. Considering the Pro_3 peptide, the data in Tables IV and V shows only one structure capable of reaching distances close to 8 Å. The single $\psi = \alpha$ structure Pro3α1 has an average distance of 9.6 Å, but the rms fluctuations of ±1.0 Å could bring the donor and acceptor to short enough distances to match the observed rate. Note that all ω = cis structures for the Pro_3 peptide have longer average donor–acceptor distances than their $\psi = \alpha$ counterparts. Note further, that neither of the structures corresponding to the recognized proline secondary structures, poly(Pro)I or Poly(Pro)II, reach distances within 5 Å of that required to reproduce the observed rate. The structure of Pro3α1, along with the extended peptide and the poly(Pro)I (all cis) structures, is shown together in Figure 8.

Turning to the Pro_4 peptide, we find three structures capable of reaching distances short enough to reproduce the observed rates: Pro4α2, Pro4α13, and Pro4α23. Again, none of the ω = cis conformations can reach the required distance, and the poly(Pro)I and poly(Pro)II secondary structures are too long by 13 and 7.5 Å, respectively. Figure 9 shows the structures of Pro4α2, Pro4α13, and Pro4α23, along with the extended (poly(Pro)II) and poly-(Pro)I structures.

Summary

We have used molecular simulations to investigate the stable conformations of proline peptides. We found kinetically stable backbone conformations with the ψ dihedral in α conformation, in addition to the recognized cis and trans isomers of the peptide ω angle. The $\psi = \alpha$ conformations are considerably more stable in simulations with explicit solvent or a dielectric constant of 80 than they are in gas-phase calculations with a dielectric of 1. We explored whether these $\psi = \alpha$ structures could change the end-to-end distance of Pro_3 and Pro_4 peptides enough to explain the electron-transfer rates observed experimentally by Isied and Vasillian.[1] We found that $\psi = \alpha$ conformations yield the shortest

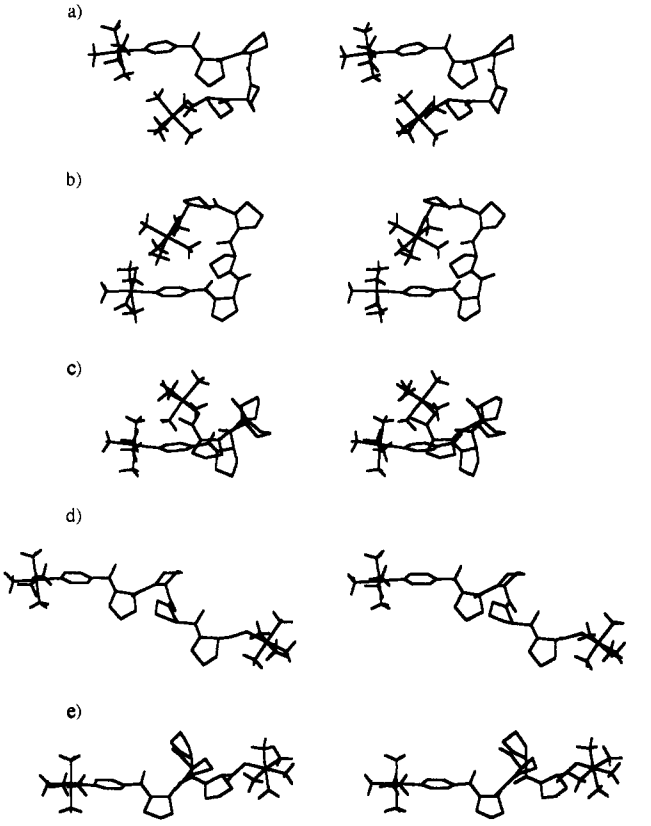

Figure 9. Stereoplots of Pro_4 structures (a) Pro4α2, (b) Pro4α13, (c) Pro4α23, (d) Pro4 extended (poly(Pro)II), and (e) Pro4 all-cis (poly-(Pro)I).

donor–acceptor distances in the Pro_3 and Pro_4 peptides and that none of the ω = cis conformations (including the all cis poly(Pro)I conformation) could reach distances short enough to explain the observed transfer rates.

The stability of proline residues with ψ in the α conformation has more general implications for the conformations of proline residues in peptides and proteins. An increasing number of instances of proline in α-helices and other α structures (e.g., reverse turns) highlights the fact that proline does not always disrupt α structures. An analysis of 50 nonhomologous high resolution proteins from the Brookhaven proteins data bank shows that approximately 40% of proline residues are in α conformation.[26,27] Of the prolines in α conformation, approximately 40% occur in α helices, with the remaining 60% roughly equally divided among 3_{10}-helices, reverse turns, and other secondary structure types.

Acknowledgment. This work was partially supported by a NIH Grant to C.L.B. (GM37554). S.F.S. received partial support from the Office of Naval Research Graduate Fellowship Program. C.L.B. is an A. P. Sloan Foundation Fellow (1990–1992). Computer time was generously provided at the Pittsburgh Supercomputing Center through the NSF and Cray Research, Inc.

Registry No. Pro1, 143142-49-8; Pro2, 143170-82-5; Pro3, 143142-50-1; Pro4, 143142-51-2.

(26) Karpen, M. E.; de Haseth, P. L.; Neet, K. E., submitted for publication.
(27) Karpen, M. E., personal communication.